

IMPACT OF MESOSCOPY ON NUCLEAR STRUCTURE PHENOMENA*

V. WERNER^{1,2}, N. COOPER², P.M. GODDARD^{2,3}, P. HUMBY^{2,3}, R.S. ILIEVA^{2,3}

¹Institut für Kernphysik, Technische Universität Darmstadt,
Schlossgartenstrasse 9, 64289 Darmstadt, Germany, EU
E-mail: vw@ikp.tu-darmstadt.de

²Wright Nuclear Structure Laboratory, Yale University,
P.O. Box 208120-8120, New Haven, CT 06520, USA

³Department of Physics, University of Surrey,
Guildford, GU2 7XH, UK

Received November 11, 2014

Results from photon-scattering experiments on ⁷⁶Se and ⁷⁶Ge are given and compared to statistical approaches, based on standard Lorentzian parametrizations.

Key words: Nuclear resonance fluorescence, collectivity,
nuclear dipole response, statistical model.

1. INTRODUCTION

The atomic nucleus displays an intriguing interplay between valence space excitations, in which relatively few nucleons in the orbits of an open shell largely define the main characteristics of the structure of the nucleus. Often excitations across shell closures, which otherwise are typically used to truncate the valence space, need to be accounted for, leading, *e.g.*, to so-called intruder configurations. Nevertheless, for heavy nuclei, the bulk of the nucleus, or its core, is neglected in the description of excitations especially at low energies.

On the other hand, well-known excitation modes are interpreted to involve the entire nuclear body. The most prominent are the so-called giant resonances [1], such as the giant dipole resonance (GDR) or giant quadrupole resonance (GQR), which are considered as oscillations of the entire proton- and neutron-bodies.

However, none of these modes are fully independent of each other - there is a coupling of valence excitations to the bulk of the nucleus. For example, consider a well deformed rotational nucleus. The deformation of the system is mainly driven by the proton-neutron (pn) interaction of the valence nucleons [2], as more and more nucleons are added to the valence space, approaching mid-shell. As a consequence, shape (phase) transitions occur between spherical nuclei near closed shells and well-deformed nuclei in the open shell. In fact, a phase diagram of nuclear shapes, akin to

*Paper presented at the conference “Advanced many-body and statistical methods in mesoscopic systems II”, September 1-5, 2014, Brasov, Romania.

that of water, has been established in the last decade [3]. These effects were clearly shown to occur in the valence space only. Nevertheless, the deformation-driving forces will influence the core and yield an overall deformation of the nuclear body. As a result, for deformed nuclei a spherical mean field is no longer applicable and deformed approaches, such as the Nilsson model [4] and use of deformed shell model bases (see, *e.g.*, Ref. [5]) are needed.

This interplay of valence space and core also manifests in simple rotational structures of deformed nuclei, as was recently pointed out [6]. *Intrinsic* excitations, such as β or γ vibrations of valence nucleons, serve as band heads of rotational structures, which in turn involve the entire nuclear body. Furthermore it has been shown [7] that it is the collective E2 excitation strengths of the lowest one-quadrupole phonon excitations, *i.e.* the pn symmetric 2_1^+ state or the mixed-symmetric $2_{1,ms}^+$ state (see review in [8]), are due to the GQR mixing into these collective valence space excitations.

Similar discussions exist for dipole excited states. In even-even nuclei, one finds low-lying $J = 1$ states, namely, the 1^+ scissors mode [9–12] and the 1^- member of the quadrupole-octupole coupled (QOC) quintuplet [13, 14]. For the scissors mode it is generally believed that its M1 excitation strength is mainly due to orbital strength within the valence space, based on systematics and correlations to the E2 excitation strength of the 2_1^+ one-phonon state [15]. However, potential admixtures of spin-flip modes have been discussed in literature (see, *e.g.*, [16]). For the QOC 1^- state there have been discussions about its E1 excitation strength, possibly originating from admixtures from the low-energy tail of the GDR.

In recent years, another dipole mode at energies intermediate between the QOC state and GDR has been discussed, the pygmy dipole resonance (PDR). In certain experiments, including photon scattering [17] or relativistic Coulomb excitation [18], an enhancement of E1 strength over the low-energy GDR tail has been observed, and a structural change of 1^- wave functions from isovector at high energies to more isoscalar character at lower energies has been found through alpha-scattering experiments in a set of nuclei (see, *e.g.*, Ref. [19]). For a recent review on the status of PDR research, see Ref. [20]. An enhancement of dipole strength at low energies - that is below or near the neutron-separation threshold in stable nuclei, but possibly above the particle threshold for exotic nuclei - could have significant consequences for the nucleosynthesis path, leading to a different equilibrium between generation and dissoziation of isotopes in a photon bath, and therefore to different results in calculations of mass abundances (see, *e.g.*, Ref. [21]).

However, the parametrization of the GDR toward low energies is not clear. Typically, Lorentzian extrapolations from GDR cross section data above the particle threshold are used. Different approaches exist, for example the use of Standard Lorentzians (SLO), potentially up to three for axially symmetric deformed or triaxial

nuclei [22], which typically only hold down to 5-6 MeV excitation energy. Other approaches, such as a Generalized Lorentzian (GLO) phenomenologically introduce a temperature dependence of the function, in order to yield a better description of observed electric dipole strengths below about 5 MeV, where SLO functions tend to overpredict data. Various other approaches exist, and in short, there is no certainty other than qualitative arguments that the one or the other strength function is correct, yet, different functions yield significantly different results in the low-energy range, where the PDR is located. A true microscopic treatment in terms of including all relevant single-particle excitations (across closed shells) is desirable, but out of reach due to the dimensions of the resulting configuration spaces. Therefore, recent approaches point in the direction of deriving photon strength functions from data, which has much improved in recent years especially below the particle threshold.

In this paper, recent results from a series of experiments on the isobars and double- β decay partners ^{76}Ge and ^{76}Se using photon-scattering will be shown and discussed in this context.

2. EXPERIMENTS

In the following the method of nuclear resonance fluorescence (NRF), as well as the laboratories and techniques used in the investigation of the dipole response of ^{76}Ge and ^{76}Se will be summarized.

2.1. BREMSSTRAHLUNG EXPERIMENTS AT THE S-DALINAC

The injector of the superconducting Darmstadt electron linear accelerator (S-DALINAC) [23] at TU Darmstadt provides intense electron beams up to about 14 MeV to the Darmstadt high-intensity photon setup (DHIPS) [24] for bremsstrahlung experiments. Figure 1 shows a schematic of the DHIPS setup, which includes the possibility for a second target assembly. The electron beam is stopped in radiator targets, which can be chosen according to the energy of the beam, in order to maximize photon production but avoid neutron release. The resulting continuous bremsstrahlung cone is then collimated through an approximately 1 m long copper tube, and subsequently impinges on the target material of interest. Typically, on the order of one gram of isotopically enriched material is required in order to achieve sufficient photo-excitation rates. The target is surrounded by HPGe detectors at 90° and 130° relative to the beam axis. At these angles angular distributions of γ -rays from decays of $J = 1$ and $J = 2$ states to the 0^+ ground state in even-even nuclei are distinctively different, hence, spin assignments can be made. The entire target and detector assembly is enclosed in lead, in order to shield the detectors against the high-radiation background in the accelerator hall.

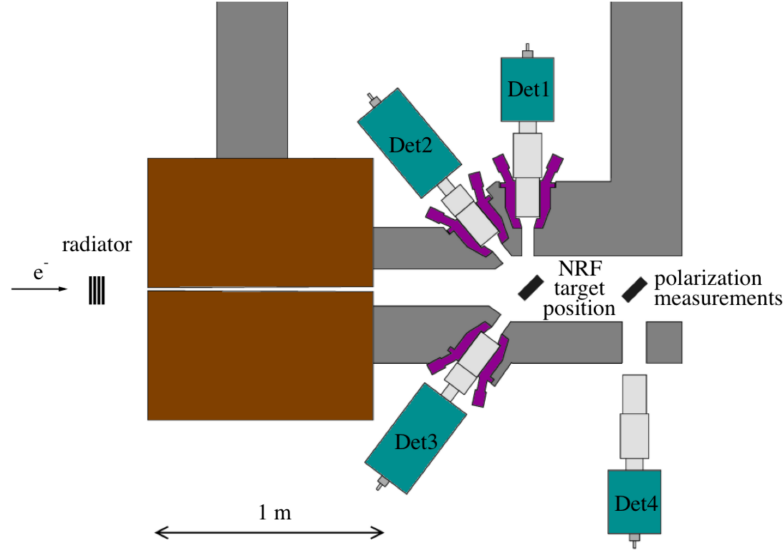


Fig. 1 – Schematic of DHIPS at the S-DALINAC facility of TU Dammstadt. The electron beam is converted to a bremsstrahlung beam in a stack of radiator targets. The bremsstrahlung is then collimated and sent to the target positions, which are surrounded by Compton-shielded HPGe detectors [24].

In the present experiments, two HPGe detectors were placed at 90° relative to the beam axis, and one at 130° . Target materials used were 4.535 g of ^{76}Se (enriched to 96,95 %) and 2.377 g of ^{76}Ge (enriched to 86 %), to which 1.244 g of ^{27}Al or 0.634 g of ^{11}B were added for photon flux calibration, depending on the chosen beam energy. ^{76}Se was measured at photon endpoint energies of 5 and 7 MeV (including ^{27}Al), and both, ^{76}Se and ^{76}Ge were measured at 9 MeV (including ^{11}B).

Target nuclei were photo-excited from their ground states with integrated cross sections of

$$I_i^S = \left(\pi \frac{\hbar c}{E_x} \right)^2 \frac{2J_x + 1}{2J_0 + 1} \frac{\Gamma_0 \Gamma_i}{\Gamma}, \quad (1)$$

where E_x is the excitation energy, $J_{x,0}$ are the excited-state and ground-state spins, respectively (*i.e.*, $J_x = 1$, $J_0 = 0$ here), Γ_i are partial decay widths from the state J_x to a lower-lying state J_i ($i = 0$ for the ground state) and Γ is the total decay width

$$\Gamma = \sum_i \Gamma_i = \frac{\hbar}{\tau}. \quad (2)$$

In continuous bremsstrahlung experiments, the integrated cross sections are extracted relative to the photon flux calibration standards. Spins of the excited states are extracted from the angular distribution ratio $R_{90/130} = W(90^\circ)/W(130^\circ)$, which takes the values of $R_{90/130} \approx 0.7$ or 2 for dipole- and quadrupole excited states, respecti-

vely. In both isotopes, nearly all states in the energy range 5 - 9 MeV were found to have $J = 1$. For most observed states only the ground state decay was observed, and consequently only the corresponding cross section I_0^S could be measured. Only in a few cases also transitions to the first or second excited 2^+ states were observed. This is typical due to the near-exponentially increasing background from non-resonant photon scattering toward lower energies. In addition, sensitivity at the highest energies was limited, because the photon flux near the endpoint energy diminishes. In order to overcome these problems, and to measure the parities of the excited states, complementary experiments were run at the HIGS facility.

2.2. BEAMS FROM COMPTON-BACKSCATTERING AT HIGS

At the HIGS facility [25] at TUNL, both isotopes, ^{76}Ge and ^{76}Se , were studied using near-monoenergetic photon beams with an energy spread of about 3 %. At HIGS, the photons are produced within a free-electron laser (FEL), and boosted to the MeV energy range through Compton-backscattering. The polarization of the FEL photons is thereby maintained and, hence, after collimation one obtains a near-100 % linearly polarized beam at the target position, only exciting states within a narrow energy interval. This allows for the determination of parities through simple polarimetry [26], and background toward lower energies is largely suppressed as compared to bremsstrahlung experiments. HPGe detectors are placed at 90° relative to the beam axis, horizontally (h) within the plane spanned by the beam and its polarization vector, and vertically (v) to that plane. Defining an asymmetry in the respective count rates,

$$P = Q \cdot \Sigma = Q \cdot \frac{N_h - N_v}{N_h + N_v}, \quad (3)$$

where $N_{h,v}$ are the respective intensities, transitions from M1 excited states to the ground state have $P = 1$, and from E1 excited states transitions have $P = -1$, somewhat attenuated due to detector solid angles, hence, the factor Q . Figure 2 shows the first results for asymmetries of ground-state decays from dipole excited states in ^{76}Ge . Most of the observed states have spin and parity 1^- . Results for ^{76}Se can be found in Refs. [27, 28].

Since the experimental sensitivity above 7 MeV was significantly higher at HIGS, several states were newly observed. Their cross sections were then deduced relative to those of neighboring states with already known cross sections, which were covered in the same beam setting. Therefore, the shape of the photon flux at the target position was simulated using GEANT4. Comparison to a spectrum taken with an additional HPGe detector placed into an attenuated beam for each beam setting ensured correct simulation of the beam profile.

Also at HIGS not all transitions to lower-lying states were directly observed. Therefore, the procedure from Ref. [29] was followed. Although many γ -ray cas-

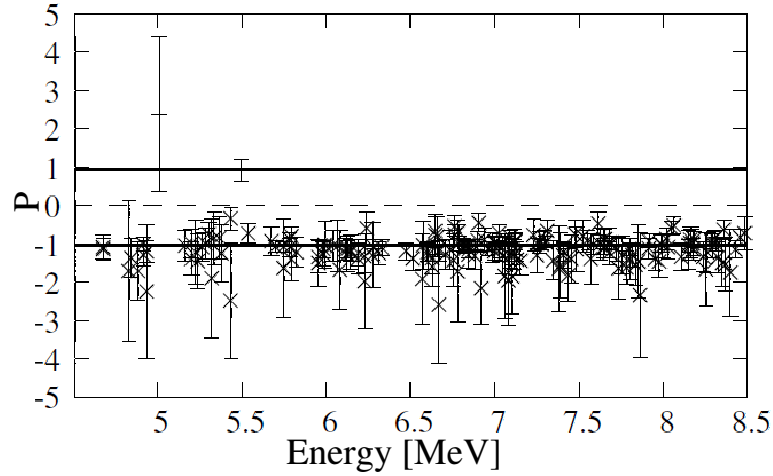


Fig. 2 – Asymmetries (P) of ground-state transitions from dipole excited states in ^{76}Ge . Lines mark the expected limits for positive and negative parity states, the dashed line marks isotropy.

cedes cannot directly be observed, one can assume that most decays pass through the first few excited 2^+ states. Therefore, the observed decays from those states can be used to obtain an average branching ratio for decays to excited states over decays to the ground state for each beam setting. The cross sections observed from ground-state transitions can then be corrected by the indirectly observed branching via

$$I_{tot}^S = I_{\Sigma,0}^S \left(1 + \sum_i \frac{N_i W_0(\theta)}{N_{\Sigma,0} W_i(\theta)} \right), \quad (4)$$

where $I_{\Sigma,0}^S$ is the sum of individual integrated ground-state decay cross sections of all states observed within the beam energy window, and $N_{\Sigma,0}$ are the respective intensities of these transitions with known angular distributions W_0 . N_i are the intensities of the observed 2^+ decays to the ground state, with angular distributions W_i , which are nearly isotropic. Results have been corrected for non-resonant absorption in the extended targets, which is considerably different for γ -rays from decays from high-lying $J = 1$ states and the low-lying 2^+ states.

3. COMPARISON OF ^{76}Ge AND ^{76}Se

As a result from the combined data from DHIPS and HIGS we obtain E1 excitation cross sections averaged over bins of 250 - 300 keV. The data from the present experiments for both isotopes are compared in Fig. 3. Also (γ, n) cross sections from experiments above the neutron threshold [30] are included. In general, the (γ, γ') data from the present work connects smoothly to the (γ, n) data. In the case of ^{76}Se ,

a slight bump may be observed in the cross sections at about 7 - 8 MeV. No such structure is visible in ^{76}Ge . Included in Fig.3 are lines that extrapolate Lorentzian fits to the GDR region to low energies, which are in fairly good agreement with data down to about 6 MeV. At energies below 6 MeV, the GDR extrapolation overshoots data, which is a typical behavior. We do not observe a clear signature of E1 strength above the low-energy tail of the GDR.

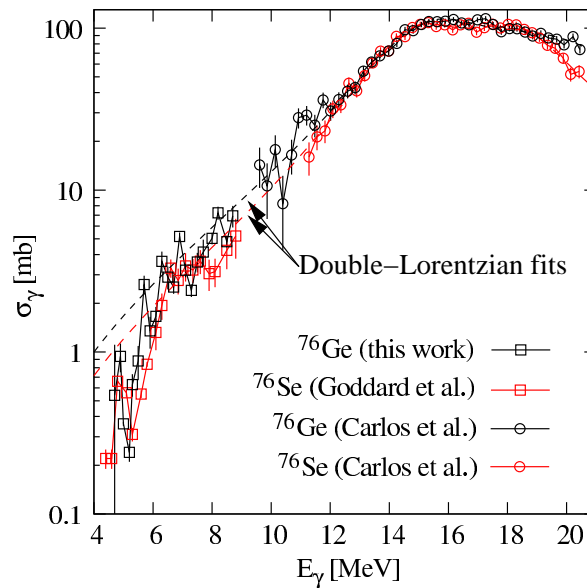


Fig. 3 – Measured E1 excitation cross sections from this work and Refs [28, 30] for ^{76}Ge and ^{76}Se . Dashed lines are fits of two Lorentzians to the GDR data above 10 MeV.

However, to quantify the E1 strength which is due to the GDR at low energies is difficult, since it requires knowledge of the E1 photon strength function (PSF), which, in general, is not known. Another question is whether the validity of the Brink hypothesis [31] can be assumed. New HIGS data on some isotopes that became available recently can serve as a test for PSFs. For example, for ^{142}Nd [32] data, in comparison to statistical calculations performed within that work, suggested that strength above the low-energy tail of the GDR was present, and that the Brink hypothesis was broken at low energies. Similar conclusions were found for ^{130}Te [33], where no trial PSF was found to consistently describe data, while for ^{78}Se [34] an iterative approach resulted in a PSF showing some enhancement over the GDR tail at about 9 MeV. One should note that there are potential systematic uncertainties in (γ, n) cross sections (see Ref. [35]) which may influence those results.

4. STATISTICAL CALCULATIONS

A new code, developed within this work, has been used to obtain a prediction of photo-excitation cross sections, based on known level schemes at low energies and simulated level schemes above a certain energy threshold. This approach involves level densities and a Wigner distribution for level spacings and a trial PSF. Average decay widths of dipole-excited states to lower-lying states are computed and then varied by Porter-Thomas Fluctuations, and the Brink hypothesis is assumed to be valid. For the calculations on ^{76}Ge and ^{76}Se a detection limit corresponding to the experimental sensitivity has been imposed on the calculations.

Simple assumptions for PSFs have been used, namely, a PSF suggested by Kadenskii, Markushev, and Furman (KMF), which was derived for the low-energy limit, and double-Lorentzian functions (SLO) fitted to GDR data. The KMF underpredicts data at higher energies, while the SLO yields an overprediction at lower energies, as mentioned above. As a compromise, we followed the approach suggested within the Ph.D. work of M. Krtička, combining the KMF and SLO PSFs with a linear cross-over around the energy where a steep rise in observed cross sections occurs. Figure 4 shows the status of these calculations in comparison to data from the ^{76}Se experiments, which are integrated over a running energy bin of 250 keV width.

In general, the combined PSF yields good agreement with data, but overshoots toward high energies. The agreement is much enhanced when taking into account an estimate for M1 strength (dashed lines in Fig. 4). Therefore, we considered a Weisskopf estimate, based on the observations in the present experiments. This assumption lowers the calculated E1 cross sections at higher energies, and results in good agreement with data.

5. CONCLUSIONS AND OUTLOOK

A series of NRF experiments using continuous unpolarized bremsstrahlung beams, as well as near-monoenergetic fully polarized photon beams, were performed on ^{76}Ge and ^{76}Se . In the present status of data analysis no enhancement of E1 strength above SLO functions fitted to available E1 response data is found. Statistical calculations show good agreement with data when assuming a combination of KMF and SLO E1 PSFs, and including an estimate for an M1 PSF. Analysis of data at energies below 5 MeV is ongoing and will complete the data sets for the entire energy range up to the neutron-separation thresholds. The present results show that it is difficult to quantify an excess of the E1 strength over the low-energy tail of the GDR, but shows that newly developed methods will allow to constrain possible PSFs, and consequently to quantify the amount of E1 strength of a PDR more reliably.

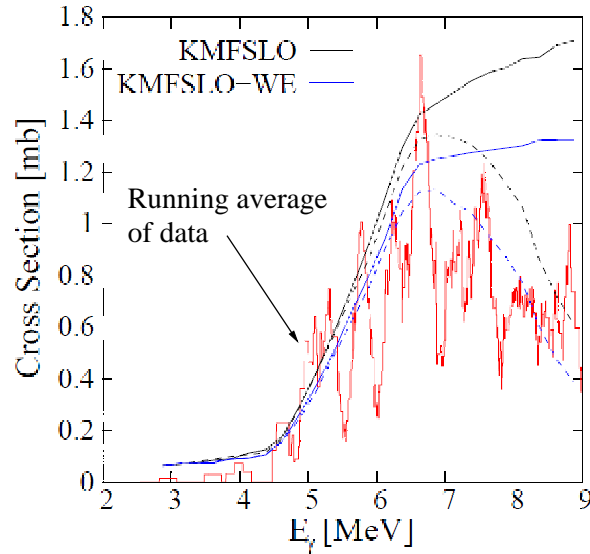


Fig. 4 – Cross sections, integrated over a running window of 250 keV width, for photo-excitation of 1^- states in ^{76}Se and decay to the ground state from data (red line). The (upper) solid black line shows the result of the statistical calculation considering only the combined KMF/SLO PSF for E1 strength. The (lower) solid blue line includes a Weisskopf estimate for M1 strengths. The respective dashed lines impose the experimental detection limit on the calculations.

The new γ^3 setup which has been employed at HIGS [36] allows to obtain γ -coincidence data after photo-excitation, and, hence, to study the decay paths of dipole-excited states in the PDR region. In addition, the advent of new facilities like ELI-NP or a possible upgrade of the HIGS facility, will give orders of magnitude higher intensities and a higher brilliance of photon beams, will allow for much higher precision studies of the PDR region, and will greatly aid the future extraction of good PSFs.

Acknowledgements. The authors acknowledge support through U.S. DOE grant Nos. DE-FG02-91ER-40609, the German BMBF grant SFB634, the UK STFC grant Nos. ST/J500768/1, ST/J00051/1, and ST/I005528/1, and the Helmholtz International Center for FAIR within the LOEWE program. We are indebted to G. Rusev for help with simulating beam conditions, and to D. Savran, N. Pietralla, and W. Tornow, as well to their respective experimental groups EMMI/GSI, TU Darmstadt, and HIGS/TUNL. We further thank E. Grosse for discussions and are grateful to the staff at the S-DALINAC and HIGS facilities for providing excellent experimental conditions.

REFERENCES

1. M.N. Harakeh and A. van der Woude, *Giant Resonances: Fundamental High-Frequency Modes of Nuclear Excitation* (Oxford University Press, Oxford, 2001).
2. R.F. Casten, *Nuclear Structure from a Simple Perspective* (Oxford University Press, Oxford, 2000).
3. D.D. Warner, *Nature* **420**, 614 (2002).
4. S.G. Nilsson *et al.*, *Nucl. Phys. A* **131**, 1 (1969).
5. K. Hara and Y. Sun, *Int. J. Mod. Phys. E* **4**, 637 (1995).
6. V. Werner, N. Pietralla, and M.K. Smith, *Eur. Phys. J. Conf.* **66**, 02109 (2014).
7. C. Walz *et al.*, *Phys. Rev. Lett.* **106**, 062501 (2011).
8. N. Pietralla, P. von Brentano, and A.F. Lisetskiy, *Prog. Part. Nucl. Phys.* **60**, 225 (2008).
9. N. Lo Iudice and F. Palumbo, *Phys. Rev. Lett.* **41**, 1532 (1978); *Nucl. Phys.* **A326**, 193 (1979).
10. F. Iachello and A. Arima, *"The Interacting Boson Model"* (Cambridge University Press, Cambridge, 1987).
11. D. Bohle *et al.*, *Phys. Lett. B* **195**, 326 (1987).
12. A. Richter, *Proc. of the Int. Conf. on Nuclear Physics*, Florence 1983, *ed.* P. Blasi and R. A. Ricci, (Tipografica Compositori Bologna, Vol. 2), p. 189.
13. C. Fransen *et al.*, *Phys. Rev. C* **57**, 129 (1998).
14. W. Andrejtscheff *et al.*, *Phys. Lett. B* **506**, 239 (2001).
15. N. Pietralla *et al.*, *Phys. Rev. C* **58**, 184 (1998).
16. D. Frekers *et al.*, *Phys. Lett. B* **218**, 439 (1989).
17. R.-D. Herzberg *et al.*, *Phys. Lett. B* **390**, 49 (1997).
18. P. Adrich, *Phys. Rev. Lett.* **95**, 132501 (2005).
19. J. Endres *et al.*, *Phys. Rev. Lett.* **105**, 212503 (2010).
20. D. Savran, T. Aumann, and A. Zilges, *Prog. Part. Nucl. Phys.* **70**, 210 (2013).
21. S. Goriely, *Phys. Lett. B* **436**, 10 (1998).
22. A.R. Junghans *et al.*, *Phys. Lett. B* **670**, 200 (2008).
23. F. Hug *et al.*, *Proc. of the 2011 Part. Acc. Conf.*, New York, NY, USA, 1999 (2011).
24. K. Sonnabend *et al.*, *Nucl. Instrum. Methods A* **640**, 6 (2011).
25. H.R. Weller *et al.*, *Prog. Part. Nucl. Phys.* **62**, 257 (2009).
26. N. Pietralla *et al.*, *Phys. Rev. Lett.* **88**, 012502 (2001).
27. N. Cooper *et al.*, *Phys. Rev. C* **86**, 034313 (2012).
28. P.M. Goddard *et al.*, *Phys. Rev. C* **88**, 064308 (2013).
29. A.P. Tonchev *et al.*, *Phys. Rev. Lett.* **104**, 072501 (2010).
30. P. Carlos *et al.*, *Nucl. Phys. A* **258**, 365 (1976).
31. D.M. Brink, Ph.D. thesis, Oxford University, 1955.
32. C.T. Angell *et al.*, *Phys. Rev. C* **86**, 051302(R) (2012).
33. J. Isaak *et al.*, *Phys. Lett. B* **727**, 361 (2013).
34. G. Schramm *et al.*, *Phys. Rev. C* **85**, 014311 (2012).
35. B.L. Berman *et al.*, *Phys. Rev. C* **36**, 1286 (1987).
36. B. Löher *et al.*, *Nucl. Instrum. Methods A* **723**, 136 (2013).